Mon. Not. R. Astron. Soc. **313**, 8–12 (2000)

Galaxy and cluster biasing from Local Group dynamics

M. Plionis,[1★] S. Basilakos,[1,2,3] M. Rowan-Robinson,[3] S. J. Maddox,[4] S. J. Oliver,[3] O. Keeble[3] and W. Saunders[5]

[1]*National Observatory of Athens, Lofos Nimfon, Thesio, 18110 Athens, Greece*
[2]*Physics Department, University of Athens, Panepistimiopolis, Greece*
[3]*Imperial College of Science, Technology and Medicine, Blackett Laboratory, Prince Consort Road, London SW1 2EZ*
[4]*School of Physics and Astronomy, University of Nottingham, Nottingham NG7 2RD*
[5]*Department of Astrophysics, Oxford University, Keble Road, Oxford OX1 3RH*

Accepted 1999 October 4. Received 1999 August 2

ABSTRACT

Comparing the gravitational acceleration induced on the Local Group of galaxies by different tracers of the underlying density field we estimate, within the linear gravitational instability theory and the linear biasing ansatz, their relative bias factors. Using optical SSRS2 galaxies, *IRAS* (PSCz) galaxies and Abell/ACO clusters, we find $b_{\rm O,I} \approx 1.21 \pm 0.06$ and $b_{\rm C,I} \approx 4.3 \pm 0.8$, in agreement with other recent studies. Finally, there is an excellent one-to-one correspondence of the PSCz and Abell/ACO cluster dipole profiles, once the latter is rescaled by $b_{\rm C,I}$, out to at least $\sim 150\,h^{-1}$ Mpc.

Key words: galaxies: clusters: general – Local Group – large-scale structure of Universe – infrared: galaxies.

1 INTRODUCTION

Different classes of extragalactic objects trace the underlying matter distribution differently. The realization of such behaviour arose from the fact that the amplitude of the two-point correlation function of clusters of galaxies is significantly higher than that of galaxies (cf. Bahcall & Soneira 1983). This was suggested by Kaiser (1984) as a result of the clustering characteristics of different height peaks in an underlying random Gaussian field. A first-order description of the effect is provided by linear biasing in which the extragalactic mass tracer fluctuation field is related to that of the underlying mass by

$$(\delta\rho/\rho)_{\rm tracer} = b(\delta\rho/\rho)_{\rm mass}, \qquad (1)$$

with b the linear bias factor. Even in this simplistic model the bias cannot be measured directly and only theoretical considerations or numerical simulations can provide some clues regarding its value. However, the relative bias between different tracers can be measured, and such attempts, using their clustering properties, have provided interesting, although somewhat conflicting, results. Lahav, Nemiroff & Piran (1990), comparing the angular correlation function of different subsamples of the UGC, ESO and *IRAS* catalogues, find an optical to IR galaxy bias factor, $b_{\rm O,I}$, ranging from 1 to 2 with preferred value $b_{\rm O,I} \sim 1.7$. Babul & Postman (1990) using the spatial correlation function of the CfA and *IRAS* galaxies, find $b_{\rm O,I} \simeq 1.2$, while comparing the QDOT correlation function (Saunders, Rowan-Robinson & Lawrence 1992) with that of APM galaxies (Maddox et al. 1990) one finds $b_{\rm O,I} \sim 1.4$. Similarly, Oliver et al. (1996), comparing the clustering properties of the Stromolo–APM survey of optical galaxies and an extended *IRAS* redshift survey, found $b_{\rm O,I} \sim 1.2 \pm 0.05$. Strauss et al. (1992a), using the 1.936-Jy *IRAS* sample, find that the overdensity ratio between CfA and *IRAS* galaxies within a sphere centred on Virgo with the Local Group (LG) on the periphery gives $b_{\rm O,I} \simeq 1.2$, while their correlation function analysis provides discrepant results when comparing *IRAS* with CfA or SSRS optical galaxies (with $b_{\rm O,I} \sim 2$ and 1, respectively). Recently, Willmer, da Costa & Pellegrini (1998), using the SSRS2 sample of optical galaxies and comparing with the clustering properties of the 1.2-Jy *IRAS* survey, find $b_{\rm O,I} \sim 1.2$ and 1.4 (± 0.07) in redshift- and real-space respectively, while Seaborne et al. (1999), performing a similar analysis between the PSC and Stromolo–APM redshift surveys, find $b_{\rm O,I} \sim 1.3 \pm 0.1$.

A different approach, using the dynamics of the Local Group of galaxies, was proposed in Plionis (1995) and Kolokotronis et al. (1996). Traditionally, dynamical studies have been used in an attempt to constrain the value of the cosmic density parameter, Ω_0, by assuming linear theory and comparing observed galaxy or cluster peculiar velocities with estimated accelerations (cf. Strauss & Willick 1995). However, owing to biasing only the combination $\Omega_0^{0.6}/b$ can be estimated. Such an analysis has been extensively applied to the Local Group of galaxies, as its peculiar velocity is accurately determined from the cosmic microwave background (CMB) temperature dipole (Kogut et al. 1993) and its gravitational acceleration can be measured from the dipole moment of the surrounding spatial distribution of different mass tracers. Within linear theory, acceleration and peculiar velocity should be aligned, and this indeed has been found to be the case using optical and IR

★ E-mail: plionis@sapfo.astro.noa.gr

galaxies, X-ray or optical cluster surveys and active galactic nuclei (cf. the reviews of Strauss & Willick 1995, Dekel 1997 and references therein). In the linear biasing framework, the different mass tracers should therefore exhibit similar dipole profiles differing only in their amplitudes, the ratio of which is a measure of their relative bias. Therefore, one can estimate the relative bias factor between different mass tracers, because in the intercomparison of their velocity–acceleration relations the Ω_0 parameter, as well as the velocity, cancels out.

In this study we use the recently completed PSCz *IRAS* galaxy survey (Saunders et al., 2000), the SSRS2 optical galaxy catalogue (da Costa et al. 1998) and a subsample of the Abell/ACO cluster catalogue (as defined in Branchini & Plionis 1996) to estimate their relative bias factors by comparing their dipole moments.

2 METHOD

Using linear perturbation theory, one can relate the gravitational acceleration of an observer, induced by the surrounding mass distribution, to her/his peculiar velocity:

$$\boldsymbol{v}(\boldsymbol{r}) = \frac{\Omega_0^{0.6}}{b}\frac{1}{4\pi}\int \delta(\boldsymbol{r})\frac{\boldsymbol{r}}{|\boldsymbol{r}|^3}\,\mathrm{d}r = \frac{\Omega_0^{0.6}}{b}\boldsymbol{D}(r). \tag{2}$$

The dipole moment, $\boldsymbol{D}$, is estimated by weighting the unit directional vector pointing to the position of each tracer, with its gravitational weight and summing over the tracer distribution:

$$\boldsymbol{D} = \frac{1}{4\pi\langle n\rangle}\sum\frac{1}{\phi(r)r^2}\hat{\boldsymbol{r}}, \tag{3}$$

with

$$\phi(r) = \frac{1}{\langle n\rangle}\int_{L_{\min}(r)}^{L_{\max}}\Phi(L)\,\mathrm{d}L, \tag{4}$$

where $\Phi(L)$ is the luminosity function of the objects under study, $L_{\min}(r) = 4\pi r^2 S_{\lim}$, with $S_{\lim}$ the flux limit of the sample and $\langle n\rangle$ is the mean tracer number density, given by integrating the luminosity function over the whole luminosity range.

Using two different tracers, i and j, of the underlying matter density field to determine the Local Group acceleration, one can write $\boldsymbol{v}(\boldsymbol{r}) = \Omega_0^{0.6}\boldsymbol{D}_i(r)/b_i = \Omega_0^{0.6}\boldsymbol{D}_j(r)/b_j$, and therefore we can obtain an estimate of their relative bias factor from

$$b_{ij}(r) = \frac{b_i}{b_j}(r) = \frac{\boldsymbol{D}_i}{\boldsymbol{D}_j}(r). \tag{5}$$

As the dipole is a cumulative quantity and at each distance it depends on all previous shells, we cannot define an unbiased χ^2 statistic to fit equation (5). Instead, we can obtain a crude estimate of the reliability of the resulting bias factor by estimating Pearson's correlation coefficient, $R_{i,j}$, between the two dipole profiles (see Kolokotronis et al. 1996); a value $R_{i,j} \simeq 1$ would indicate a perfect match of the two dipole profiles and thus a very reliable estimate of their relative linear bias factor.

A statistically more reliable approach is to assume that the differential dipoles, estimated in equal volume shells, are independent of each other and then fit b_{ij} according to

$$\chi^2 = \sum_{k=1}^{N_{\rm bins}}\frac{(\boldsymbol{D}_{i,k} - b_{ij}\boldsymbol{D}_{j,k} - \mathcal{C}_k)^2}{\sigma_{i,k}^2 + b_{ij}^2\sigma_{j,k}^2}, \tag{6}$$

where $\mathcal{C}$ is the zero-point offset of the relation and σ is the corresponding shot-noise error, estimated by using either of two methods: a Monte Carlo approach in which the angular coordinates of all tracers are randomized while keeping their distance, and thus their selection function, unchanged, or the analytic estimation of Strauss et al. (1992b) [$\sigma^2 \simeq \sum\phi^{-1}r^{-4}(\phi^{-1}+1)$].

3 DATA

We use in our analysis three different catalogues of mass tracers:

(i) The recently completed *IRAS* flux-limited 60-μm redshift survey (PSCz), which is described in Saunders et al. (2000). It is based on the *IRAS* Point Source Catalogue and contains ∼15 000 galaxies with flux >0.6 Jy. The subsample we use, defined by $|b| \geqslant 10^\circ$ and a limiting galaxy distance of $180\,h^{-1}$ Mpc, contains ∼10 097 galaxies and covers ∼82 per cent of the sky.

(ii) The SSRS2 catalogue of optical galaxies (da Costa et al. 1998), which is magnitude-limited to $m_B = 15.5$ and contains 3573 galaxies in the south ($-40^\circ \leqslant \delta \leqslant -2.5^\circ$, $b \leqslant -40^\circ$) and 1939 galaxies in the north ($\delta \leqslant 0^\circ$, $b \geqslant 35^\circ$), covering in total 13.5 per cent of the sky.

(iii) A volume-limited subsample of the Abell/ACO cluster catalogue, with $|b| \geqslant 10^\circ$ and limited within $180\,h^{-1}$ Mpc (see Branchini & Plionis 1996). Our sample contains 197 clusters.

3.1 Determining distances from redshifts

All heliocentric redshifts are first transformed to the Local Group frame using $cz \simeq c\,z_\odot + 300\sin(l)\cos(b)$. We then derive the distance of each tracer by using

$$r = \frac{2c}{H_0}[1 - (1 + z - \delta z)^{-1/2}](1 + z - \delta z)^{3/2}, \tag{7}$$

where $H_0 = 100\,h$ Mpc and δz is a non-linear term to correct the redshifts for the tracer peculiar velocities:

$$\delta z = \frac{1}{c}[\boldsymbol{u}(r) - \boldsymbol{u}(0)]\cdot\hat{r}, \tag{8}$$

with $\boldsymbol{u}(0)$ the peculiar velocity of the Local Group and $\boldsymbol{u}(r)$ the peculiar velocity of a galaxy or cluster at position $\boldsymbol{r}$. Instead of using elaborate 3D reconstruction schemes (cf. Schmoldt et al. 1999; Branchini & Plionis 1996; Branchini et al. 1999a; Rowan-Robinson et al. 1999) to estimate this term, we decided to use a rather simplistic velocity field model (see Basilakos & Plionis 1998) to treat all three data sets consistently (a self-consistent 3D reconstruction of the SSRS2 density field is in any case not possible because of the small area covered by the survey). Our simplistic velocity field model was found in Basilakos & Plionis (1998) to be sufficient in order to recover the *IRAS* 1.2-Jy and QDOT 3D dipole. We remind the reader of the main assumptions of this model.

(i) The tracer peculiar velocities can be split into two vector components, those of a bulk flow and a local non-linear term:

$$\boldsymbol{u}(r) = \boldsymbol{V}_{\rm bulk}(r) + \boldsymbol{u}_{\rm nl}(r). \tag{9}$$

(ii) The first component dominates, and thus

$$\boldsymbol{u}(r)\cdot\hat{\boldsymbol{r}} \approx \boldsymbol{V}_{\rm bulk}(r)\cdot\hat{\boldsymbol{r}}. \tag{10}$$

We then use the observed bulk flow direction and profile, as a function of distance, given by Dekel (1997) and combined with

that of Branchini, Plionis & Sciama (1996). The zero-point, $V_{\rm bulk}(0)$, and the direction of the bulk flow is estimated applying equation (9) at $r = 0$ and assuming, because of the 'coldness' of the local velocity field (cf. Peebles 1988), that $\boldsymbol{u}_{\rm nl}(0) \simeq \boldsymbol{u}_{\rm inf} = 200\,{\rm km\,s^{-1}}$ (where $u_{\rm inf}$ is the LG infall velocity to the Virgo Supercluster).

3.2 Galaxy densities

To estimate the local acceleration field it is necessary to recover the true galaxy density field from the observed flux-limited samples. This is done by weighting each galaxy by $\phi^{-1}(r)$, where $\phi(r)$ is defined in equation (4). For the PSCz sample we use the Saunders et al. (1990) luminosity function derived from the QDOT catalogue, with $L_{\rm min} = 7.5 \times 10^7\, h^{-2}\,{\rm L}_\odot$, because lower luminosity galaxies are not represented well in the available samples (cf. Rowan-Robinson et al. 1990), and $L_{\rm max} = 10^{13}\, h^{-2}\,{\rm L}_\odot$. For the SSRS2 sample we use the Schechter luminosity function of Marzke et al. (1998) with $M_{\rm max} = -22$ and $M_{\rm min} = -13.8$.

In Fig. 1 we present the mean density and its Poissonian uncertainty of PSCz and SSRS2 galaxies in their common area (that of the SSRS2 sample) and in equal volume shells (with $\delta V \simeq 4.5 \times 10^6\, h^{-3}\,{\rm Mpc}^3$). Their densities are extremely comparable, differing only by a constant factor $(\langle\rho_{\rm O}\rangle/\langle\rho_{\rm I}\rangle = 2.03 \pm 0.16)$.

4 RESULTS

4.1 Optical to IR galaxy bias

We first present the results of the intercomparison of the SSRS2 and PSCz samples in their common sky area and for $r \geqslant 15\,h^{-1}\,{\rm Mpc}$. In Fig. 2(a) we show the amplitudes of the two dipoles as a function of distance from the LG. The monotonic dipole increase reflects the fact that we are measuring only the component of the whole sky dipole that comes from the particular area covered by the sky-restricted SSRS2 sample. It is apparent that the shapes of the two dipole amplitudes are extremely similar, giving correlation coefficient $R \simeq 0.97$.

In Fig. 2(b) we present the direct dipole ratio (equation 5) in the LG frame (open symbols), while the results of the fit of equation (6), as a function of maximum distance used, are displayed as filled squares. No significant differences are found when correcting distances for peculiar velocities. It is evident that the different estimates are consistent with each other, especially for $r > 50\,h^{-1}\,{\rm Mpc}$ where the direct dipole ratio becomes flat. It is essential, however, to verify whether such a good dipole-profile correlation could result solely from the small solid angle used, i.e. to investigate whether the survey geometry, coupled with the galaxy selection function, dominates the dipole signal of both samples. To this end we have generated 100 mock SSRS2 samples by reshuffling the galaxy angular coordinates while leaving their distances, and thus selection function, unchanged. If the reshuffled dipole profile resembles that of the SSRS2 original one, then this would indicate the existence of the previously suggested bias. In Fig. 3 we present both (a) the dipole ratio between the original SSRS2 dipole and the reshuffled one together with its scatter and (b) the SSRS2 and PSCz dipole ratio with the latter rescaled by $b_{\rm O,I}$. It is evident that the former ratio deviates significantly from 1, an indication that our comparison is not dominated by the suspected bias.

Using the differential equal volume dipoles to fit equation (6) for $10 \leqslant r \leqslant 185\,h^{-1}\,{\rm Mpc}$, we find $b_{\rm O,I} \simeq 1.24 \pm 0.04$, with zero-point $\mathcal{C} \simeq -105 \pm 50\,{\rm km\,s^{-1}}$ and $\chi^2 \approx 6.3$ for 6 degrees of freedom. The fit is performed using the FITEXY routine of Press

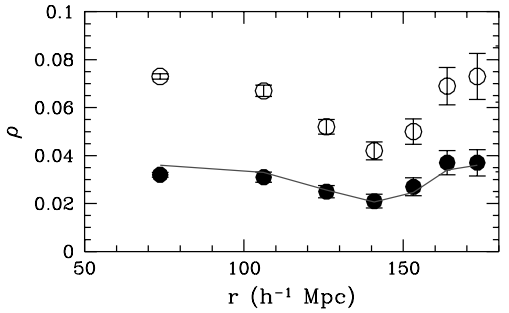

Figure 1. Mean SSRS2 (open symbols) and PSCz (filled symbols) galaxy space density estimated in equal-volume shells with its Poissonian uncertainty. The continuous line is the SSRS2 density reduced by a factor of 2. Based on 13.5 per cent of the sky (SSRS2 survey area).

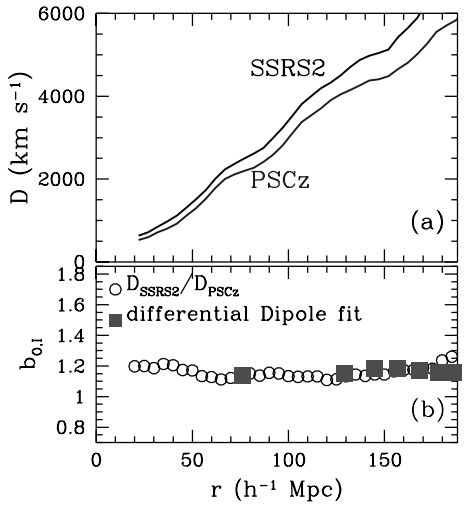

Figure 2. (a) Dipole amplitude comparison for the SSRS2 and PSCz samples. (b) The estimated bias from comparing cumulative dipoles using equation (5) (open circles) and differential dipoles using equation (6) (filled squares).

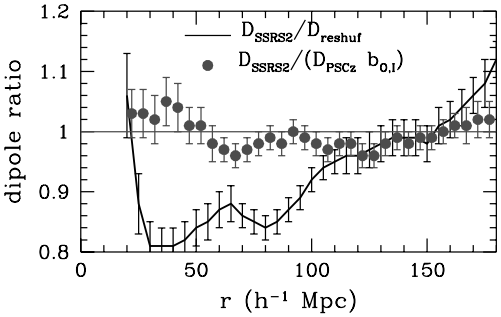

Figure 3. Cumulative dipole ratio test. The solid line represents the ratio of the original SSRS2 and mean reshuffled dipoles, with its scatter estimated over 100 reshufflings of the galaxy angular coordinates. Solid points represent the ratio of the SSRS2 and PSCz dipoles, with the latter rescaled by $b_{\rm O,I} \simeq 1.17$ (see text), while the errors represents the propagation of the shot-noise dipoles.

et al. (1992) and the uncertainties of the fitted parameters correspond to the $\Delta\chi^2 = 1$ confidence region boundary. The small zero-point offset could be caused by uncertainties in tracing the very local contributions to the LG dipole. Indeed, integrating the the SSRS2 and PSCz dipoles for $r > 15\,h^{-1}$ Mpc (presented in Fig. 2) we find no zero-point offset $\mathcal{C} \simeq -40 \pm 45\,\mathrm{km\,s^{-1}}$ but a slightly smaller bias factor $b_{\mathrm{O,I}} \simeq 1.17 \pm 0.04$, with $\chi^2 \approx 7.5$ for 6 degrees of freedom. We derive a mean estimate of the bias factor and its uncertainty by varying both the inner and outer dipole integration limits in equation (5) and by taking into account the slight differences of the results based on the differential dipole (equation 5). The resulting optical to IR galaxy bias factor is

$$b_{\mathrm{O,I}} \simeq 1.21 \pm 0.06.$$

Our result is in quite good agreement (within 1σ) with that of Seaborne et al. (1999), which is based on the PSCz and APM galaxy clustering properties on relatively smaller scales than those probed by our dipole analysis.

4.2 Rich cluster to IR galaxy bias

In the case of the cluster and PSCz samples we have a nearly full sky coverage, except at low galactic latitudes. In order to recover the whole sky dipole we use a spherical harmonic approach to 'fill' the unobserved part of the sky (cf. Lahav 1987; Plionis & Valdarnini 1991). This approach has been found to provide compatible results with the cloning and interpolating method (see Branchini & Plionis 1996 for such a comparison in the context of the cluster dipole).

The main drawback of comparing the cluster and galaxy dipoles arises from the fact that the Abell/ACO cluster distribution is incomplete in the local universe, because it does not include the Virgo cluster, an important contributor of the local velocity field (cf. Tully & Shaya 1984). Therefore the direct comparison of the dipole amplitudes is hampered by this zero-point uncertainty. We can attempt to correct for this problem by

(i) including the local Virgo contribution to the cluster dipole by assigning an appropriate Abell number count (N_{A}) weight to the Virgo cluster;

(ii) excluding from the PSCz dipole the very near contributions ($\lesssim 8\,h^{-1}$ Mpc).

A first attempt to derive the cluster to IR galaxy bias, using such a procedure and the Abell/ACO and QDOT catalogues, was presented by Plionis (1995). If clusters and galaxies do trace the same underlying field, as indeed appears to be the case (cf. Branchini et al. 1999a,b), then we should be able to fit the two profiles, using equation (6), varying the Virgo cluster weight. The appropriate value of N_{A} is that for which the zero-point, $\mathcal{C}$, of the fit vanishes and thus we will consider as our preferred bias parameter the corresponding value of $b_{\mathrm{C,I}}$. Statistically, this procedure does not provide a rigorous significance indication, owing to the fact that the dipoles are cumulative quantities, but it provides a means of comparing quantitatively the two dipole profiles. In order to test the robustness of the resulting bias parameter we fit the two dipole profiles as a function of distance.

In Fig. 4(a) we present the resulting bias parameter versus the zero-point, $\mathcal{C}$, for the Virgo cluster weights that provide a fit with $\mathcal{C} \approx 0$. The different connected point arrays correspond to results based on the different N_{A} weights while different points in each array correspond to different upper distance limits used for the fit, which increase as indicated by the arrow. Taking into account that

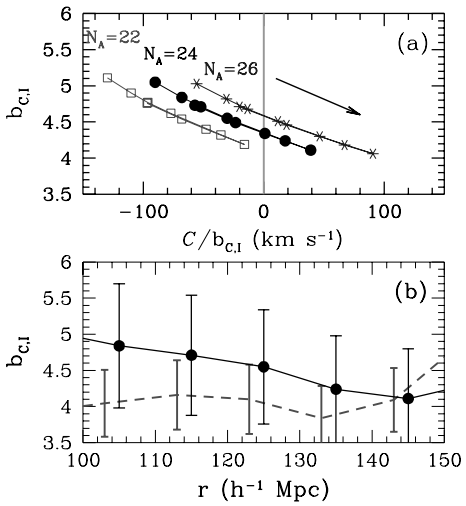

Figure 4. (a) Fitted bias parameter between clusters and *IRAS* galaxies versus zero-point, $\mathcal{C}$, for different Virgo cluster weights. The different points within each connected array represent the results of the fit to different limiting distances (increasing in the direction of the arrow). (b) The fitted bias parameter (equation 6) as a function of limiting distance for $N_{\mathrm{A}} = 24$ (continuous line). The broken line is the corresponding direct dipole ratio (equation 5).

the zero-point uncertainty is $\delta\mathcal{C} \simeq 130\,\mathrm{km\,s^{-1}}$, we conclude that the Virgo cluster weight for which $\mathcal{C} \approx 0$ is $N_{\mathrm{A}} = 24 \pm 4$, confirming the notion that Virgo corresponds to a richness class $R = 0$ Abell cluster. A consistency check, which we pass with success, is that the Virgocentric infall velocity, that corresponds to this weight, is $u_{\mathrm{inf}} \simeq 300 \pm 40\,\mathrm{km\,s^{-1}}$, a value in agreement with most available determinations.

In Fig. 4(b) we present the fitted bias parameter as a function of upper distance limit (points) and the direct dipole ratio (equation 5) as broken lines for the $N_{\mathrm{A}} = 24$ case. Both seem consistent within their uncertainties, especially for distances $\sim$140–150 h^{-1} Mpc, which roughly corresponds to the apparent cluster dipole convergence depth.

The main result regarding the bias parameter is

$$b_{\mathrm{C,I}} \simeq 4.3 \pm 0.8,$$

which interestingly is mostly independent of the Virgo cluster weights (as can be seen in Fig. 4a), because such differences are absorbed in the value of $\mathcal{C}$. The uncertainty in $b_{\mathrm{C,I}}$ reflects (a) variations caused by different Virgo weights, (b) the variation between the equation (5) and equation (6) solutions and (c) the scatter around these solutions (see Fig. 4b). It does not include, however, the cosmic variance that results from the use of only one observer. Our results are in excellent agreement with those of Peacock & Dodds (1994) and Branchini et al. (1999b) based on completely different approaches.

In Fig. 5 we present a direct comparison of the PSCz and Abell/ACO cluster dipoles, out to $150\,h^{-1}$ Mpc, after having scaled down the latter by $b_{\mathrm{C,I}} = 4.3$. The error bars in the cluster dipole reflect mainly the uncertainty of the cluster density between the Abell and ACO parts of the sample (see Plionis & Kolokotronis 1998 and references therein). The two profiles are in excellent agreement, at least up to $\sim 150\,h^{-1}$ Mpc with correlation coefficient $R = 0.86$. This is a further indication that the two density fields are consistent with each other out to these distances and supports the existence of dipole contributions from large

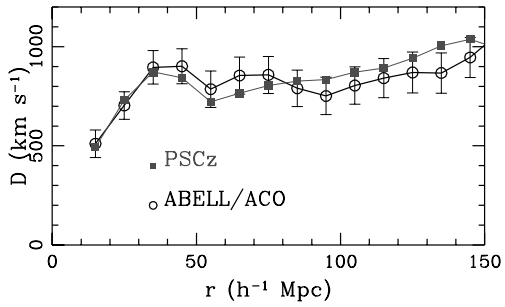

Figure 5. Comparison between the PSCz and ABELL/ACO dipoles, after scaling down the latter by a bias factor of 4.3.

depths (see also Schmoldt et al. 1999; Basilakos & Plionis 1998), suggestions that were first put forward by Plionis (1988), on the basis of the Lick counts, by Rowan-Robinson et al. (1990) on the basis of the QDOT survey and by Scaramella, Vettolani & Zamorani (1991) and Plionis & Valdarnini (1991) on the basis of Abell/ACO clusters. A thorough investigation of the deep PSCz dipole (distances $>150\,h^{-1}$ Mpc) is presented in Rowan-Robinson et al. (1999).

5 CONCLUSIONS

We have used a novel approach, based on the Local Group dipole properties, to estimate the relative bias parameter of different mass tracers. We find that the optical to IR galaxy bias parameter is $b_{\rm O,I} \simeq 1.21 \pm 0.06$, while the rich cluster to IR galaxy bias is $b_{\rm C,I} \simeq 4.3 \pm 0.8$. Our results are in good agreement with others based on different approaches. We find that the IR galaxy and rich cluster dipole profiles are extremely compatible once the latter is rescaled by $b_{\rm C,I}$ out to at least $\sim 150\,h^{-1}$ Mpc.

ACKNOWLEDGMENTS

SB thanks the Greek State Fellowship Foundation for financial support (Contract No 2669). We thank V. Kolokotronis for useful comments.

REFERENCES

Babul A., Postman M., 1990, ApJ, 359, 280
Bahcall N., Soneira R., 1983, ApJ, 270, 20
Basilakos S., Plionis M., 1998, MNRAS, 299, 637
Branchini E., Plionis M., 1996, ApJ, 460, 569
Branchini E., Plionis M., Sciama D. W., 1996, ApJ, 461, L17
Branchini E. et al., 1999a, MNRAS, 308, 1
Branchini E., Zehavi I., Plionis M., Dekel A., 1999b, MNRAS, in press
da Costa L. N. et al., 1998, AJ, 116, 1
Dekel A., 1997, in da Costa L., Renzini A., eds, Galaxy Scaling Relations: Origins, Evolution and Applications. Springer, Berlin, p. 245
Kaiser N., 1984, ApJ, 284, L9
Kogut A. et al., 1993, ApJ, 419, 1
Kolokotronis V., Plionis M., Coles P., Borgani S., Moscardini L., 1996, MNRAS, 280, 186
Lahav O., Nemiroff J., Piran T., 1990, ApJ, 350, 119
Lahav O., 1987, MNRAS, 225, 213
Maddox S. J., Efstathiou G., Sutherland W. J., Loveday J., 1990, MNRAS, 242, 43P
Marzke R. O., da Costa L. N., Pellegrini P. S., Willmer N. A., Geller M. J., 1998, ApJ, 503, 617
Oliver S. J. et al., 1996, MNRAS, 280, 673
Peacock J. A., Dodds S. J., 1994, MNRAS, 267, 1020
Peebles P. J. E., 1988, ApJ, 332, 17
Press W. H., Teukolsky S. A., Vetterling W. T., Flannery B. P., 1992, Numerical Recipes, 2nd edn. Cambridge Univ. Press, Cambridge
Plionis M., 1988, MNRAS, 234, 401
Plionis M., 1995, in Maurogordato S., Balkowski C., Tao C., Trân Thanh Vân J., eds, Proc. Moriond Meeting on Clustering in the Universe. Editions Frontieres, Gif-sur-Yvette, p. 273
Plionis M., Valdarnini R., 1991, MNRAS, 249, 46
Plionis M., Kolokotronis V., 1998, ApJ, 500, 1
Rowan-Robinson M. et al., 1990, MNRAS, 247, 1
Rowan-Robinson M. et al., 1999, preprint (astro-ph/9912223)
Saunders W., Rowan-Robinson M., Lawrence A., Efstathiou G., Kaiser N., Ellis R. S., Frenk C. S., 1990, MNRAS, 242, 318
Saunders W., Rowan-Robinson M., Lawrence A., 1992, MNRAS, 258, 134
Saunders W. et al., 2000, preprint (astro-ph/0001117)
Scaramella R., Vettolani G., Zamorani G., 1991, ApJ, 376, L1
Schmoldt I. et al., 1999, MNRAS, 304, 893
Seaborne M. D. et al., 1999, MNRAS, 309, 89
Strauss M. A., Willick J. A., 1995, Phys. Rep., 261, 271
Strauss M. A., Davis M., Yahil A., Huchra J. P., 1992a, ApJ, 385, 421
Strauss M. A., Yahil A., Davis M., Huchra J. P., Fisher K., 1992b, ApJ, 397, 395
Tully R. B., Shaya E. J., 1984, ApJ, 281, 31
Willmer C. A., da Costa L. N., Pellegrini P. S., 1998, AJ, 11, 869

This paper has been typeset from a TEX/LATEX file prepared by the author.